Available online at www.sciencedirect.com
SCIENCE DIRECT®
Catalysis Today 99 (2005) 123–129
CATALYSIS TODAY
www.elsevier.com/locate/cattod

Structure–reactivity relationships in supported VO_x catalysts for the oxyhydrative scission (OHS) of 1-butene and *n*-butane to acetic acid A comprehensive catalytic and in situ study

A. Brückner[a,*], U. Bentrup[a], M. Fait[a], B. Kubias[b]

[a]*Institut für Angewandte Chemie Berlin-Adlershof, P.O. Box 961156, D-12474 Berlin, Germany*
[b]*Department of Inorganic Chemistry, Fritz-Haber-Institut, Faraday-Weg 4-6, D-14195 Berlin, Germany*

Available online 15 December 2004

Abstract

A pure and an antimony-modified VO_x/TiO_2 catalyst have been catalytically tested in a total pressure range of 1–17 bar and studied by in situ FTIR, in situ UV/vis and operando-EPR spectroscopy at normal pressure in the oxyhydrative scission (OHS) of 1-butene and *n*-butane to acetic acid (AA). While 1-butene OHS follows the sequence butene → butoxide → ketone → acetate/AA with a multitude of trace side products also formed, *n*-butane OHS leads to AA, CO_x and H_2O only. Adding water to the feed improves AA selectivity by favouring the hydrolysis of the ketone intermediate. Doping by Sb was found to improve AA selectivity being due, among other reasons, to deeper V reduction under steady-state conditions. Activity in *n*-butane OHS decreases continuously with rising total pressure while both activity and selectivity in 1-butene OHS pass a maximum at 7 bar.

Keywords: In situ FTIR; Operando-EPR; In situ UV/vis-DRS; Oxyhydrative scission; 1-Butene; *n*-Butane; Vanadia–titania catalysts

1. Introduction

The industrial production of light olefins is based on naphtha cracking. In this process, considerable amounts of *n*-butenes and butane are formed as side products. Many attempts have been made in the past to convert these cheap and abundant raw materials to valuable products. Besides dehydrogenation to butadiene, selective oxidation to maleic anhydride (MA) is an established industrial process [1]. In recent years, a new process has been developed for small to medium plants that converts the butadiene-free raffinate II fraction containing a mixture of 80% *n*-butene and 20% *n*-butane by oxyhydrative scission to acetic acid (AA) whereby AA selectivities of about 65 mol% are achieved [2]. So far, mixed vanadium/titanium oxides appeared to be most promising catalysts for this process, in particular, when they are additionally modified by oxides of antimony, chromium or molybdenum [2–5]. However, a serious problem is that of the two C_4 hydrocarbons, *n*-butane is converted with a markedly lower rate. For making this process economically more attractive it is, thus, a major challenge to develop catalysts and optimize reaction conditions in such a way that effective conversion of *n*-butane to AA is ensured while maintaining a satisfactory performance for the butene-to-AA transformation. For reaching this goal, a deep understanding of structure–reactivity relationships in this catalytic system is required. Thus, previous studies have shown that the pathway of butene oxidation depends strongly on the acid–base properties of the catalysts [6,7]. It was found that, on acidic surfaces, butene is converted to strongly adsorbed O-containing intermediates such as butoxy and butanone species that react with water to form AA and acetaldehyde [6,7], while on basic catalysts oxydehydrogenation products resulting from allylic intermediates are preferably formed [1,6]. Furthermore, it was shown by ‘‘operando spectroscopy’’ (a name recently introduced for spectroscopic monitoring of active sites and determination of catalytic performance in the same single experiment [8]) combining EPR/UV–vis/on line-GC measurements that the dispersion

* Corresponding author. Tel.: +49 30 6392 4301; fax: +49 30 6392 4454.
E-mail address: brueckner@aca-berlin.de (A. Brückner).

0920-5861/$ – see front matter © 2004 Elsevier B.V. All rights reserved.
doi:10.1016/j.cattod.2004.09.031

and behavior of V sites in supported vanadia catalysts is of crucial importance for the selectivity in the selective oxidation of light alkanes [9].

Against this background, it is the aim of this work to derive detailed information on the mode of interaction of *n*-butane and *n*-butene with the catalyst components as well as on the influence of different reaction conditions on the performance of a VO_x/TiO_2 catalyst in the oxyhydrative scission (OHS) of C_4 hydrocarbons. This was done by combining catalytic tests in a wide range of reaction conditions with comprehensive catalyst characterization under reaction like conditions using FTIR, EPR and UV–vis spectroscopy. In particular, the influence of total pressure and the role of water vapour added to the feed have been studied to evaluate reaction conditions similar to those applied in industry.

2. Experimental

Experiments were performed with two catalysts provided by Consortium für Elektrochemische Industrie (Munich). They have been prepared by spray-drying of a slurry of V_2O_5 and TiO_2 (V/Ti) or V_2O_5, Sb_2O_3 and TiO_2 (V/Sb/Ti) and following calcination in air at 400 °C. Catalyst V/Ti (S_{BET}: 79 m^2/g) contains 6.1 wt.% V. Catalyst V/Sb/Ti (S_{BET}: 74 m^2/g) contains 4.2 wt.% V and 9.5 wt.% Sb. As support material, a sulfate-doped TiO_2 with anatase modification was used. By XRD, only weak peaks of V_2O_5 in addition to typical reflections of anatase have been detected in sample V/Ti while clearly visible peaks of Sb_2O_3 but no peaks of V_2O_5 are evident in the powder pattern of V/Sb/Ti [10]. In contrast, large crystallites of V_2O_5 have been detected by TEM/EDX in both catalysts [10] illustrating the limited sensitivity of XRD for small amounts of V_2O_5.

In situ FTIR spectra were recorded from self-supporting wafers (Ø = 20 mm, m = 60 mg) using a Bruker IFS 66 spectrometer equipped with a heatable and evacuable IR cell with CaF_2 windows, connected to a gas dosing-evacuation system. After oxidative pretreatment for 30 min at 400 °C in air flow, samples were treated at different temperatures in flowing reactant gas mixtures of the following composition: 5 vol.% HC/N_2, 3 vol.% HC, 8 vol.% O_2/N_2 and 3 vol.% HC, 8 vol.% O_2, 3 vol.% H_2O/N_2 (HC = 1-butene or *n*-butane). Water was added by using a saturator.

EPR spectra in X-band ($\nu \approx 9.5$ GHz) were recorded by the cw-spectrometer ELEXSYS 500-10/12 (Bruker) using a microwave power of 6.3 mW, a modulation frequency of 100 kHz, and a modulation amplitude of 0.5 mT. For operando experiments, i.e., recording of EPR spectra at reaction temperatures between 180 and 200 °C in flowing reactant gas mixtures combined with simultaneous product analysis in the same single experiment, a home-made flow reactor connected to a gas/liquid-supplying system containing mass-flow controllers and a saturator was used [11]. This reactor was loaded with 200 mg catalyst particles (d = 0.2–0.3 mm) and directly implemented into the rectangular EPR cavity. For on-line activity measurements, the reactor outlet was connected to a GC 17AAF gas chromatograph (Shimadzu) equipped with a 25 m × 0.32 mm CP 7747 capillary column (Chrompack). Before entering the GC, the product stream was led through a cold trap filled with water at 0 °C to remove water-soluble products.

A UV/VIS Carry 400 spectrometer (Varian) equipped with a diffuse reflectance accessory (type praying mantis, Harrick) and a respective flow cell (Harrick) was used to determine the reduction/reoxidation kinetics of the catalyst by following the absorbance at 600 nm as a function of time. This wavelength is characteristic for d–d transitions of reduced vanadium species [12]. To reduce light absorption, catalysts were diluted in a ratio of 1:10 with α-Al_2O_3 which had been calcined at 1400 °C for 4 h. Experimental values were fitted by a pseudo-first-order rate law using Eq. (1):

$$\mathrm{Abs}_t = \mathrm{Abs}_{t=\infty} + (\mathrm{Abs}_{t=0} - \mathrm{Abs}_{t=\infty})\, e^{-kt} \quad (1)$$

in which $\mathrm{Abs}_{t=0}$, Abs_t and $\mathrm{Abs}_{t=\infty}$ are the absorbance values at 600 nm at the start of the experiment, at time t and after reaching steady state, respectively. Samples were pretreated in O_2 flow (5 ml/min) at 200 °C for 2 h until a constant value of absorbance at 600 nm was reached. Then the gas flow was changed to 5 vol.% 1-butene or *n*-butane, respectively, in N_2 (15 ml/min) and maintained for 3 h. Reoxidation was done by switching back to O_2 flow at 200 °C and maintaining for 3 h.

Catalytic tests were performed with catalyst granules of 1.25–2.5 mm diameter using a fixed-bed tube reactor of 11 mm diameter operating in the temperature range from 160 to 220 °C. The feed mixture contained 1.9 vol.% 1-butene or *n*-butane, respectively, 9.1 vol.% O_2 and usually 24.4% water vapour in N_2. The influence of total pressure was studied in the range 1–17 bar at a constant GHSV (NPT) of 3730 h^{-1} for 1-butene (0.7 g catalyst) and 74 h^{-1} for *n*-butane (41.2 g catalyst). To investigate the effect of water vapour in the feed, the vapour concentration was varied between 6.1 and 24.4 vol.% using the V/Sb/Ti catalyst at 185 °C and 7 bar total pressure. In these experiments, GHSV (NPT) for *n*-butane containing feed was varied between 160 and 600 h^{-1} to maintain a constant conversion of 20 and 25%, respectively. In the case of 1-butene, the dependence of conversion and AA selectivity on water concentration was studied using a constant GHSV (NPT) = 3730 h^{-1}.

Product compositions were analyzed by on line-GC (GC 17A, Shimadzu) at normal pressure. After pre-separation of butane and butenes/butadiene, respectively, from water and oxygenates (column: CP-WAX 52 CBDF 0.50, Varian Chrompack), *n*-butenes, *n*-butane and butadiene were analyzed by a HP-Plot Al_2O_3 column (HP) and a flame ionization detector. Water and oxygenates (formic acid, acetic acid, propionic acid, acetaldehyde) were separated by a Stabilwax-DA column (Restek) and detected by a thermal

conductivity detector. CO_x was analyzed by non-dispersive IR photometry and O_2 by a solid-state electrolyte cell (Infralyt 40, Junkalor, Germany). Conversion degrees and selectivities were calculated with respect to C_4 concentration in the feed gas. The feed and product concentrations were balanced on the carbon basis (100 ± 4%).

3. Results and discussion

3.1. Operando-EPR studies

Before studying the interaction of feed components with the catalysts, the latter have been pretreated in air flow for 1 h at 200 °C. The room-temperature spectra of these pre-oxidized catalysts are rather similar showing a weak signal with partially resolved hyperfine structure that arises from highly dispersed VO^{2+} persisting the oxidative pretreatment (Fig. 1).

Upon switching to a flow of 3% 1-butene, 8% O_2/N_2 (total flow: 20 ml/min), the intensity of the EPR signal increases immediately already at room temperature for both catalysts (Fig. 1A and C). This shows clearly that pentavalent VO_x species are reduced to VO^{2+} species to a considerable extent. The poorly resolved hyperfine structure indicates furthermore that those species are no longer isolated but coupled by magnetic interactions.

The signal of VO^{2+} in sample V/Ti increases during the whole reaction period at 200 °C (Fig. 1C). During this time, 1-butene conversion remains roughly constant. Sample V/Sb/Ti shows a very similar behavior in the initial period of the experiment. However, in contrast to sample V/Ti, the VO^{2+} signal intensity does not further increase with time-on-stream at 200 °C and 1-butene conversion drops quickly (Fig. 1A) which is due to the accumulation of hydrocarbon deposits on the surface (identified by FTIR) that are probably formed by polymerization. Moreover, the line-width of the EPR signal of sample V/Sb/Ti is larger than for sample V/Ti and the hyperfine structure is still partly resolved after 4.5 h time-on-stream, suggesting that the VO^{2+} sites formed under reaction conditions might be more separated than in sample V/Ti. When both catalysts are exposed to ambient atmosphere after finishing the operando experiment, the intensity of the VO^{2+} EPR signal in catalyst V/Ti remains almost unchanged while it increases by about 20% in catalyst V/Sb/Ti. This suggests that, in contrast to sample V/Ti the V valence of which does not drop below +4, catalyst V/Sb/Ti might contain a certain amount of V^{3+} formed during reaction which is oxidized to VO^{2+} in air.

When *n*-butane is used as a substrate instead of 1-butene on the V/Sb/Ti catalyst, a much smaller VO^{2+} EPR signal is formed during reaction (Fig. 1B) suggesting that the working catalyst remains more oxidized than in the presence of 1-butene. Moreover, while fast deactivation is observed with 1-butene, this does not occur with *n*-butane. In situ FTIR measurements described below have shown that, with butane, no adsorbed intermediates are accumulated on the surface and AA is the only product, the desorption of which might be favoured by the acidic nature of the surface. This could suppress deactivation by surface deposit formation as observed in feed mixtures containing 1-butene.

When adding water vapour to the 1-butene feed as it is done similarly under industrial conditions, the EPR spectra of the V/Ti catalyst do not differ much in the initial period of the experiment (compare Fig. 1C and D). However, with increasing time-on-stream, the VO^{2+} EPR signal broadens and a partially resolved hyperfine structure appears indicating a weakening of magnetic interactions between

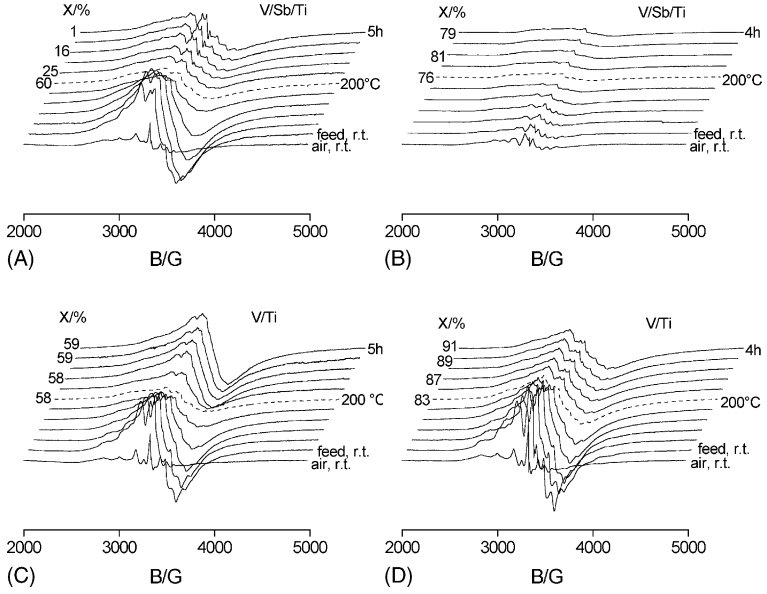

Fig. 1. In situ EPR spectra of: (A) V/Sb/Ti in a flow of 3% 1-butene, 8% O_2/N_2, (B) V/Sb/Ti in a flow of 2.2% *n*-butane, 10% O_2/N_2, (C) V/Ti in a flow of 3% 1-butene, 8% O_2/N_2, and (D) V/Ti in a flow of 3% 1-butene, 8% O_2, 24.4% H_2O/N_2 as well as corresponding conversions at 200 °C.

VO^{2+} formed during reaction. This suggests that water might favour spreading of VO_x species and, thus, lower the size of VO_x agglomerates.

3.2. In situ FTIR studies

Upon treating the catalysts at room temperature in a flow of 3 vol.% 1-butene/N_2 or 3 vol.% 1-butene, 8 vol.% O_2/N_2, bands of adsorbed 1-butene at 1633 and 1616 cm^{-1} from ν(C=C) and around 1460 cm^{-1} from δ_{as}(–CH_3) and δ(–CH_2) modes [13] are observed in the in situ FTIR spectra (not shown) [10]. Additional bands around 1660 and 1560 cm^{-1} being most pronounced for adsorption of 1-butene only are due to ν(C=O) of adsorbed ketone and an adsorbed enolate species, respectively, which is formed by acid-catalyzed enolization of ketones [14]. These results show clearly that lattice oxygen species bound to the V sites participate in the oxidation of 1-butene by which the latter are reduced to some extent. In 1-butene/O_2/N_2 flow, less surface adsorbates and oxygenated species are detected due to a continuously working Mars–van Krevelen-like redox cycle which causes fast further oxidation to products that can easily desorb from the catalyst surface. Generally, both catalysts show similar behavior despite a slightly higher overall spectra intensity of sample V/Ti that points to a higher surface concentration of adsorbed products and intermediates in comparison to catalyst V/Sb/Ti.

At 200 °C bands of adsorbed 1-butene are no longer observed due to its fast reaction to adsorbed ketone (ν(C=O) at 1655 cm^{-1} [14]) and acetate species (ν_{as} and ν_s(COO^-) at 1540 and 1441 cm^{-1} [14]) (Fig. 2A). With increasing time on stream bands at 1620 and 1780 cm^{-1} (ν(C=C) and ν(C=O)) gain intensity. They are assigned to adsorbed cyclic anhydrides [15,16] formed by oxidation of butadiene [17] which itself may be regarded as dehydrogenation product of 1-butene [18].

Adding water vapour to the feed leads in principle to the formation of the same species (Fig. 2B). However, essentially less cyclic anhydride species are formed suggesting that water blocks adsorption sites and might selectively suppress the side reaction leading to cyclic anhydride formation.

When 1-butene is replaced by *n*-butane, the FTIR spectra are dominated by ν(C=O) bands around 1653 cm^{-1} (adsorbed AA) and ν(COO^-) bands at 1530 and 1450 cm^{-1} from acetate species while bands of ν(C=C) and cyclic anhydride disappear almost completely in the case of V/Sb/Ti sample (Fig. 3). This shows clearly that the undesired side reaction, i.e. dehydrogenation and further oxidation to cyclic anhydrides, plays a negligible role.

3.3. Redox kinetics studied by UV/vis-DRS

From in situ EPR experiments described above, it is evident that V^{5+} species are reduced by 1-butene and *n*-butane to a different extent. The equilibrium valence state of the V sites in steady state is expected to depend on the rate of reduction/reoxidation steps under reaction conditions. Therefore, the redox kinetics of both catalysts has been studied in the presence of 1-butene and *n*-butane. To fit experimental values properly, two pseudo-first-order processes had to be assumed for both reduction and reoxidation, a fast process for the initial period from 0 to 20 min reflected by rate constant k_1 and a slow process from 20 to 180 min reflected by rate constant k_2 (Table 1). It is probable that the fast process comprises VO_x species on the surface that are readily exposed to reactants while the slow process might be related to VO_x sites in deeper layers, e.g., in the volume of the V_2O_5 particles. By comparing the rate constants k_1 and k_2 in Table 1, it is evident that the two catalysts do not differ much in their redox behavior when using the same reducing agent, although the k_1 values ascribed to reoxidation of surface V sites are slightly higher for the Sb-containing

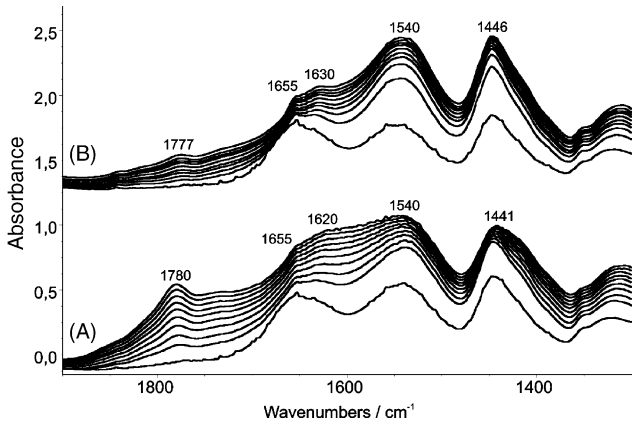

Fig. 2. FTIR spectra of adsorbates formed on V/Ti during reaction of: (A) 3% 1-butene, 8% O_2/N_2 and (B) 3% 1-butene, 8% O_2, 3% H_2O at 200 °C. First spectrum after 1 min contact time, following spectra each after 10 min from bottom to top.

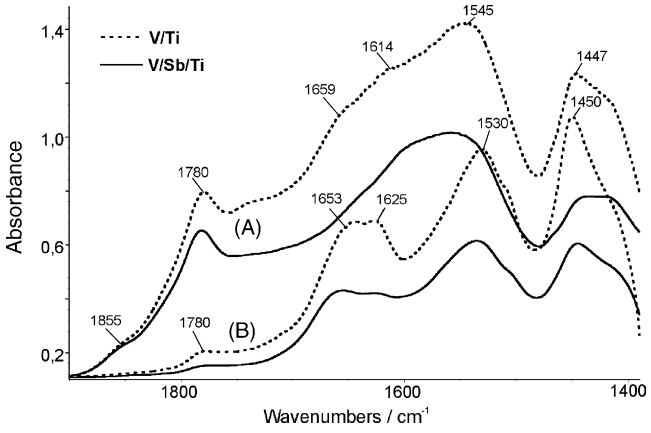

Fig. 3. FTIR spectra of adsorbates formed on V/Ti and V/Sb/Ti during reaction of: (A) 3% 1-butene, 8% O_2/N_2 and (B) 3% *n*-butane, 8% O_2/N_2 at 200 °C. Spectra after 90 min reaction time, cooling to ambient temperature and evacuation.

Table 1
Pseudo-first-order rate constants (10^{-3} min^{-1}) for reduction of V^{5+} in a flow of 5% 1-butene/N_2 or 5% *n*-butane/N_2, respectively, and reoxidation in O_2

	Reduction		Reoxidation	
	V/Ti	V/Sb/Ti	V/Ti	V/Sb/Ti
k_1(1-butene)	172	186	187	239
k_2(1-butene)	11	9	16	14
k_1(*n*-butane)	85	83	143	159
k_2(*n*-butane)	12	26	18	15

k_1 and k_2 were derived by fitting the experimental curve from 0 to 20 and 20 to 180 min, respectively.

catalyst suggesting that Sb could accelerate the reoxidation of those sites.

However, as seen from Table 1, the difference between 1-butene and *n*-butane is well visible. In the case of 1-butene, rate constants for reduction and reoxidation for each of the two processes are similar. When *n*-butane is used, the reoxidation rate constants are in the same order of magnitude than with 1-butene. However, surface reduction with *n*-butane is markedly slower than surface reduction with 1-butene (compare k_1 in Table 1). This is in proper agreement with operando-EPR results (Section 3.1) revealing a markedly deeper reduction of the catalyst in the presence of 1-butene and with in situ FTIR results (Section 3.2) confirming the formation of more oxygen-containing surface adsorbates in the latter case. Moreover, the total extent of reduction reflected by the difference of absorbance at 600 nm in the UV–vis spectra before and after 3 h treatment in C_4/N_2 is markedly higher in the case of 1-butene (Δabs(V/Ti) = 0.080, Δabs(V/Sb/Ti) = 0.062) than with *n*-butane (Δabs(V/Ti) = 0.037, Δabs(V/Sb/Ti) = 0.039).

3.4. Catalytic tests

The performance of the two catalysts in OHS of 1-butene at ambient pressure is shown in Fig. 4. While the activity of V/Ti and V/Sb/Ti does not differ much, the latter catalyst is significantly more selective. Taking the above-described FTIR results into account which revealed a lower concentration of adsorbates on the surface of sample V/Sb/Ti, it seems probable that the higher selectivity of this catalyst arises from facilitated desorption of products which suppresses total oxidation. In addition to AA being the main product, formic acid, acetaldehyde and propionic acid (selectivities: 1–14%, not shown in Fig. 4) are formed as valuable by-products besides 25 further trace components (mono- and dicarboxylic acids (MA), carbonyl compounds, alcohols, esters).

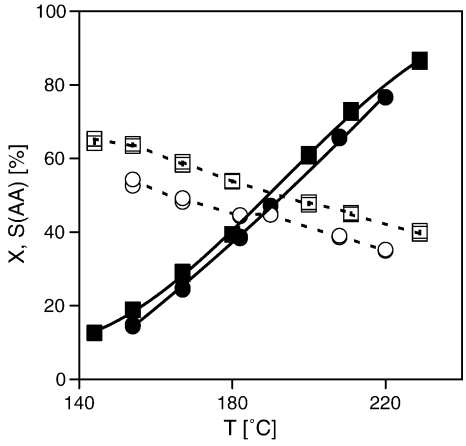

Fig. 4. 1-Butene conversion (filled symbols) and acetic acid selectivity (open symbols) as a function of catalyst temperature for sample V/Ti (circles) and V/Sb/Ti (squares) at normal pressure (feed: 1.9% 1-butene, 9.1% O_2, 24.4% H_2O/N_2).

When *n*-butane is used as substrate, residence times must be increased by a factor of about 50 to reach conversion degrees comparable to the more reactive substrate butene. However, in contrast to the latter, only AA, carbon oxides and water are formed as products when butane is oxidized.

Under industrial conditions, OHS of butane and butene is performed at elevated total pressure. Thus, catalytic tests have been done for sample V/Sb/Ti with both substrates at total pressures varying between 1 and 17 bar for elucidating optimum reaction conditions. In the case of 1-butene, both conversion and AA selectivity pass a maximum at 7 bar suggesting this total pressure value as an optimum for highest catalytic performance (Fig. 5A). When butane is used as a substrate, conversion drops continuously above 3 bar while AA selectivity remains almost constant over the whole pressure range studied (Fig. 5B).

The effect of total pressure on the hydrocarbon consumption rates related to the mass of catalyst is also shown in Fig. 5. In 1-butene OHS, a saturation effect is observed at pressures above 7 bar while the hydrocarbon consumption rate increases continuously with rising pressure in butane OHS. This points to a strong interaction of 1-butene with the catalyst surface which leads to an autoinhibition in analogy to results obtained in the oxidation of butene and butadiene over VPO catalysts [19]. In contrast, the interaction of butane with the catalyst surface is weak and, therefore, does not cause autoinhibition of the reaction. The loss of AA selectivity in the butene oxidation at 17 bar (Fig. 5A) could be caused by non-selective electrophilic oxygen species that may gain importance due to the growing coverage of the surface with strongly adsorbed butene and water molecules at higher pressure which hinder the fast conversion of the adsorbed oxygen species into lattice oxygen.

Differences in the interaction of olefin and alkane with the catalyst surface are also evident from results obtained with different water content in the feed at 185 °C and a total pressure of 7 bar (Fig. 6). For 1-butene, the mass-related consumption rate decreases continuously with increasing water vapour concentration (Fig. 6A) while AA selectivity increases. This might be due to the increasing displacement of 1-butene from the surface by water which competes with 1-butene for the same adsorption sites. With increasing concentration, water vapour inhibits the adsorption of 1-butene but facilitates AA desorption thus preventing AA from further oxidation and leading to improved selectivity.

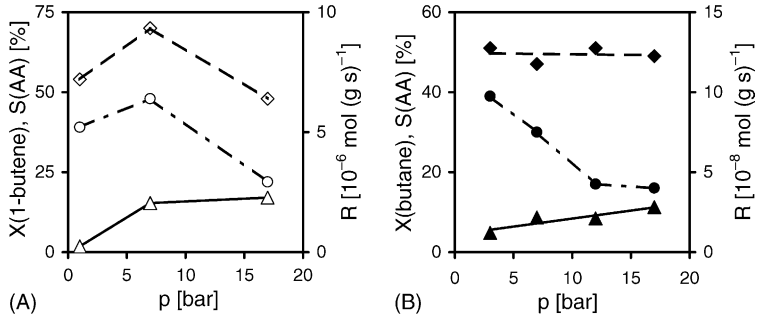

Fig. 5. Conversion degrees (circles), acetic acid selectivities (squares) and relative rates of hydrocarbon consumption related to the catalyst mass (triangles) for sample V/Sb/Ti at 180 °C as a function of total pressure for 1-butene OHS (A) (GHSV (NPT) = 3730 h^{-1} = const.) and *n*-butane OHS (B) (GHSV (NPT) = 74 h^{-1} = const., feed: 1.9% HC, 9.1% O_2, 24.4% H_2O/N_2).

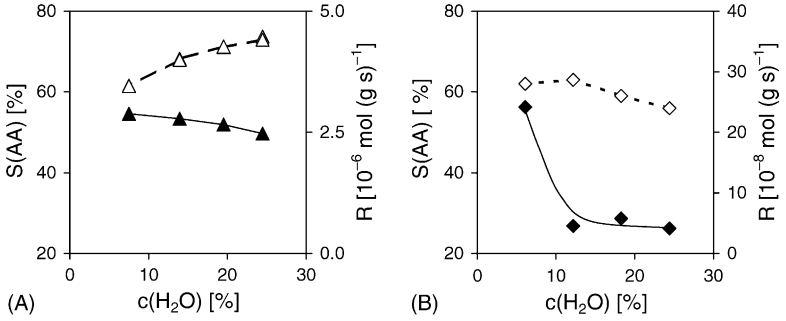

Fig. 6. Relative rates of hydrocarbon consumption related to the catalyst mass (filled symbols) and acetic acid selectivity (open symbols) for sample V/Sb/Ti (185 °C, 7 bar) as a function of water vapour concentration of 1-butene OHS (A) (GHSV (NPT) = 3730 h^{-1} = const.) and *n*-butane OHS (B) (GHSV (NPT) has been varied to maintain a constant *n*-butane conversion of 20%), feed in both cases: 1.9% HC, 9.1% $O_2/H_2O/N_2$.

When butane is used as a substrate, the mass-related consumption rate decreases sharply with rising water concentration reaching a constant low level above 10% (Fig. 6B) since water adsorption is considerably favoured in comparison to butane adsorption. The observed decrease of AA selectivity with increasing water concentration might be due to an overcompensation of the selectivity-enhancing AA desorption by water vapour due to reaction of the above-mentioned non-selective oxygen species that might gain importance under these reaction conditions.

4. Conclusions

The in situ experiments performed in this work show clearly that the OHS of both 1-butene and *n*-butane over V/Ti and V/Sb/Ti catalysts proceeds via a Mars–van Krevelen redox mechanism comprising cyclic reduction and reoxidation of active V sites. Due to the higher reactivity of 1-butene being directly reflected in the catalytic tests, the vanadium component of both catalysts is deeper reduced than with *n*-butane in steady state, whereby the mean V valence in V/Ti does probably not drop below +4 while a certain amount of V^{3+} is obviously formed in sample V/Sb/Ti. This V^{3+} might be located within an amorphous non-stoichiometric $SbVO_4$-like phase for which hints have been obtained by TEM/EDX measurements presented in [10]. In such a phase, the mean V valence is generally lower than +4 and can vary between 3.2 and 3.8 depending on the pretreatment procedure [20]. Due to the presence of such a component, the mean V valence in the initial sample V/Sb/Ti might be lower than in the initial sample V/Ti. This could also be the reason why the total extent of reduction reflected by the difference of absorbance at 600 nm in the UV–vis spectra before and after 3 h treatment in 1-butene/N_2 flow is lower for sample V/Ti/Sb than for sample V/Ti, since it is not likely that V^{3+} in the former sample is even deeper reduced.

Partial reduction to V^{3+} lowers the redox potential of the active V sites. This in turn could be the reason for higher AA selectivities observed with V/Sb/Ti in the OHS of 1-butene. Another beneficial effect for higher AA selectivity could arise from Sb doping which is known to enhance the surface acidity of the catalysts, thus, facilitating AA desorption [10]. Moreover, the slightly higher reoxidation constant k_1 measured for sample V/Ti/Sb (Table 1) suggests that Sb favours the reoxidation of surface V sites in a $SbVO_4$-like phase. This could be the reason why sample V/Sb/Ti does not loose activity in comparison to catalyst V/Ti although the average V valence in steady state should be lower than in V/Ti.

In situ FTIR studies of 1-butene revealed that the reaction leads via the sequence 1-butene → butoxide → ketone → acetate to acetic acid as the main product and to a minor extent via dehydrogenation and further oxidation to cyclic anhydride (most probably maleic anhydride) and CO_x, finally. Catalytic tests revealed that the substrate 1-butene and these main products/intermediates are partially also transformed to a multitude of trace products such as mono- and dicarboxylic acids, maleic anhydride, carbonyl compounds, alcohols and esters. AA selectivity was found to be improved with rising water content in the feed. As revealed by in situ FTIR measurements, water supports the conversion of adsorbed acetate into acetic acid which can desorb from the surface. On the other hand, the dispersion of active VO_x seems to be favoured, too, in the presence of water. Both effects might be beneficial for AA selectivity. However, the water content should not exceed a certain limit (ca. 12%) at a total pressure of 7 bar to avoid extensive blocking of adsorption sites and, as a consequence, dropping conversions.

Remarkably, no products besides AA, CO_x and H_2O are formed with *n*-butane which is an advantage with respect to product separation and purification. Unfortunately, the reactivity of *n*-butane is much lower in comparison to 1-butene and this difference does not decrease at elevated total pressure as usually applied in the industrial process [2]. By varying the reaction conditions (temperature, total pressure, water vapour content) no suitable set of process parameters could be found that allows to narrow the activity gap of the catalysts for simultaneous OHS of butene and butane. From this, the principal dilemma of the process is readily evident: attempts to optimize reaction conditions for simultaneous OHS of butene and butane seem to be hopeless, leaving behind catalyst modification (e.g., by doping with suitable elements) as the only possible way to improve the process for raffinate II conversion. Alternatively, the development of a process based on *n*-butane oxidation only seems promising.

Acknowledgements

We thank C. Rüdinger and H.-J. Eberle (Consortium für Elektrochemische Industrie GmbH) for providing catalysts as well as the German Federal Ministry of Education and Research for financial support (Grant No. 03C0323).

References

[1] G. Centi, F. Trifiro, J.R. Ebner, V.M. Franchetti, Chem. Rev. 88 (1988) 55.
[2] C. Rüdinger, H.-J. Eberle, Consortium f. Elektrochem. Industrie GmbH, EP 0960,874 (1999); US 6,281,385 (2001).
[3] Y. Takita, K. Nita, T. Maehara, N. Yamazoe, T. Seiyama, J. Catal. 50 (1977) 364.
[4] W.E. Slinkard, P.B. DeGroot, J. Catal. 68 (1981) 423.
[5] T. Ono, T. Mukai, H. Miyata, T. Ohno, F. Hatayama, Appl. Catal. 49 (1989) 273.
[6] G. Busca, V. Lorenzelli, J. Chem. Soc., Faraday Trans. 88 (1992) 2783.
[7] G. Busca, E. Finocchio, V. Lorenzelli, G. Ramis, M. Baldi, Catal. Today 49 (1999) 453.
[8] B.M. Weckhuysen, Chem. Commun. (2002) 97.
[9] A. Brückner, P. Rybarczyk, H. Kosslick, G.-U. Wolf, M. Baerns, Stud. Surf. Sci. Catal. 142B (2002) 1141.
[10] U. Bentrup, A. Brückner, C. Rüdinger, H.-J. Eberle, Appl. Catal. A: Gen. 269 (2004) 237.
[11] A. Brückner, B. Kubias, B. Lücke, R. Stößer, Colloid. Surf. 115 (1996) 179.
[12] C.J. Ballhausen, H.B. Gray, Inorg. Chem. 1 (1962) 111.
[13] G. Busca, G. Ramis, V. Lorenzelli, A. Janin, J.-C. Lavalley, Spectrochim. Acta 43A (1987) 489.
[14] V.S. Escribano, G. Busca, V. Lorenzelli, J. Phys. Chem. 95 (1991) 5541.
[15] G. Socrates, Infrared and Raman Characteristic Group Frequencies, Wiley, Chichester, 2001, p. 129/130.
[16] G. Ramis, G. Busca, V. Lorenzelli, J. Mol. Catal. 55 (1989) 1.
[17] G.C. Bond, A.J. Sarkani, G.D. Parfitt, J. Catal. 57 (1979) 476.
[18] G. Busca, Catal. Today 27 (1996) 457.
[19] F. Cavani, G. Centi, I. Manenti, A. Riva, F. Trifirò, Ind. Eng. Chem. Prod. Res. Dev. 22 (1983) 565.
[20] A. Landa-Canovas, J. Nilsson, S. Hansen, K. Stahl, A. Andersson, J. Solid State Chem. 116 (1995) 369.